Two-dimensional Organic Semiconductor-incorporated Perovskite (OSiP) Electronics

Wenchao Zhao[1,2], Sheng-Ning Hsu[1], Bryan W. Boudouris[1,3], Letian Dou[1,4]*

[1] Charles D. Davidson School of Chemical Engineering, Purdue University, West Lafayette, IN 47907, USA

[2]Co-Innovation Center of Efficient Processing and Utilization of Forest Resources, College of Materials Science and Engineering, Nanjing Forestry University, Nanjing, 210037, China

[3] Department of Chemistry, Purdue University, West Lafayette, IN 47907, USA

[4] Birck Nanotechnology Center, Purdue University, West Lafayette, IN 47907, USA

AUTHOR INFORMATION

Corresponding Author

*Letian Dou: dou10@purdue.edu

KEYWORDS: organic semiconductors, halide perovskite, field-effect transistor, thermoelectric device, memory device

ABSTRACT

Two-dimensional organic semiconductor-incorporated perovskites (OSiPs) are an emerging family of hybrid optoelectronically-active materials. Their inherent quantum-well structures, tunable electronic properties, and excellent environmental stability make them promising for next-generation solution-processed electronic devices. In this spotlight article, we provide a brief introduction to OSiP materials and critically review the recent progress of these materials and their applications in electronic modules, such as field-effect transistors, thermoelectric energy conversion devices, and memory devices. Finally, we discuss the current challenges and opportunities regarding the future of OSiPs materials and related electronic devices.

1. INTRODUCTION

Halide perovskites are an intriguing class of solution-processable semiconducting materials that have gained enormous attention due to their high performance in a variety of devices.[1-3] For example, halide perovskite photovoltaics and light-emitting diodes have achieved tremendous success in the last few years.[4, 5] While most research efforts in halide perovskites focus on optoelectronics, studying their properties and applications in non-optical electronics, such as field-effect transistors (FETs), thermoelectric modules, and memory devices, are equally important.[6-8] In addition, halide perovskite-based electronics serve as useful platforms to probe their electronic and charge transport properties, which is important for designing new materials for enhanced performance.

Similar to optoelectronics, several material stability issues of halide perovskites have hampered their adoption in practical non-optical electronics. For example, ion migration that occurs under large electric fields, which adversely impacts the performance of FETs. Additionally, their thermal stability, which is essential for thermoelectric applications, also needs to be

improved. To overcome these stability issues in halide perovskites and boost the performance of these electronic devices, two-dimensional (i.e., 2D or layered) halide perovskites are proposed as a potential solution.[9-11] Within the family of 2D halide perovskites, a number of groups, including our own, have focused on incorporating semiconducting organic building blocks in the ligands to enhance the charge transport between the organic and inorganic layers and their stability simultaneously.[12-15] This class of materials, known as organic semiconductor-incorporated perovskites (OSiPs), provides a promising pathway to overcome these pressing challenges in the perovskite community.[16, 17] In this spotlight article, we focus on the recent progress of OSiPs and their applications in electronic devices. In addition, we provide a short perspective on promising future applications in different electronic devices. We believe that OSiPs are a new and useful materials platform for elucidating the charge transport properties of hybrid materials, and they have the potential to revolutionize the next generation of low-cost, high-performance, lightweight, and flexible electronic systems.

2. STRUCTURES

Halide perovskites have a general formula of ABX_3, where A is a monovalent cation such as cesium or methylammonium (MA), B is a divalent metal cation (Pb^{2+} or Sn^{2+}), and X is a halide anion (Cl^-, Br^-, or I^-). These materials suffer from poor stability upon exposure to: illumination, moderate temperatures (e.g., over 100 °C), moisture, and/or electric fields.[18] Conversely, 2D halide perovskites are considered a potential solution to these instability issues. Furthermore, the quantum and dielectric confinement effects associated with 2D halide perovskites result in unique optical and electrical properties.[10, 19] Among 2D perovskites, the Ruddlesden-Popper phase (RP phase) is the most studied due to its robustness with respect to ligand chemistry (**Figure 1a)**. The RP phase has a general formula of $L_2A_{n-1}B_nX_{3n+1}$, in which L is a bulky monovalent cation. Common

examples are electrically inactive long-chain organic cations like phenylethylammonium (PEA), and butylammonium (BA). The variable n indicates the number of metal halide octahedral layers encapsulated between the two layers of the L cations. By changing the n variable, the thickness of the inorganic sheet can be modified to fine-tune their optical and electronic properties. The stability of the 2D perovskites originates from higher formation energy and the hydrophobicity of the organic spacers that protect the air and moisture-sensitive inorganic layers.[20, 21] Importantly, the structural tunability and the intrinsic stability of 2D perovskite offers an opportunity to achieve high-performance and stable halide perovskite electronics.

Introducing the 2D structure largely enhances the environmental stability of halide perovskites. On the other hand, the bulky ligands usually hamper charge transport due to the insulating nature of the ligand molecular design. Inspired by the great success of organic semiconductors, π-conjugated ligands were developed and incorporated into the 2D perovskite structures (i.e. OSiPs) to overcome the charge transport across the bulky ligand layers.[13-15] OSiPs not only show improved charge transport properties, but they also have significantly improved chemical and thermal stability as the π-conjugated ligands greatly suppress ion migration.[22, 23] Because many comprehensive reviews on optoelectronics (e.g. photovoltaics and LEDs) have been published in recently,[19, 24-27] we focus on the non-optical electronics of OSiPs. A few representative structures of the ligands used in OSiPs electronic devices are listed in **Figure 1b**.[12, 14, 28-31]

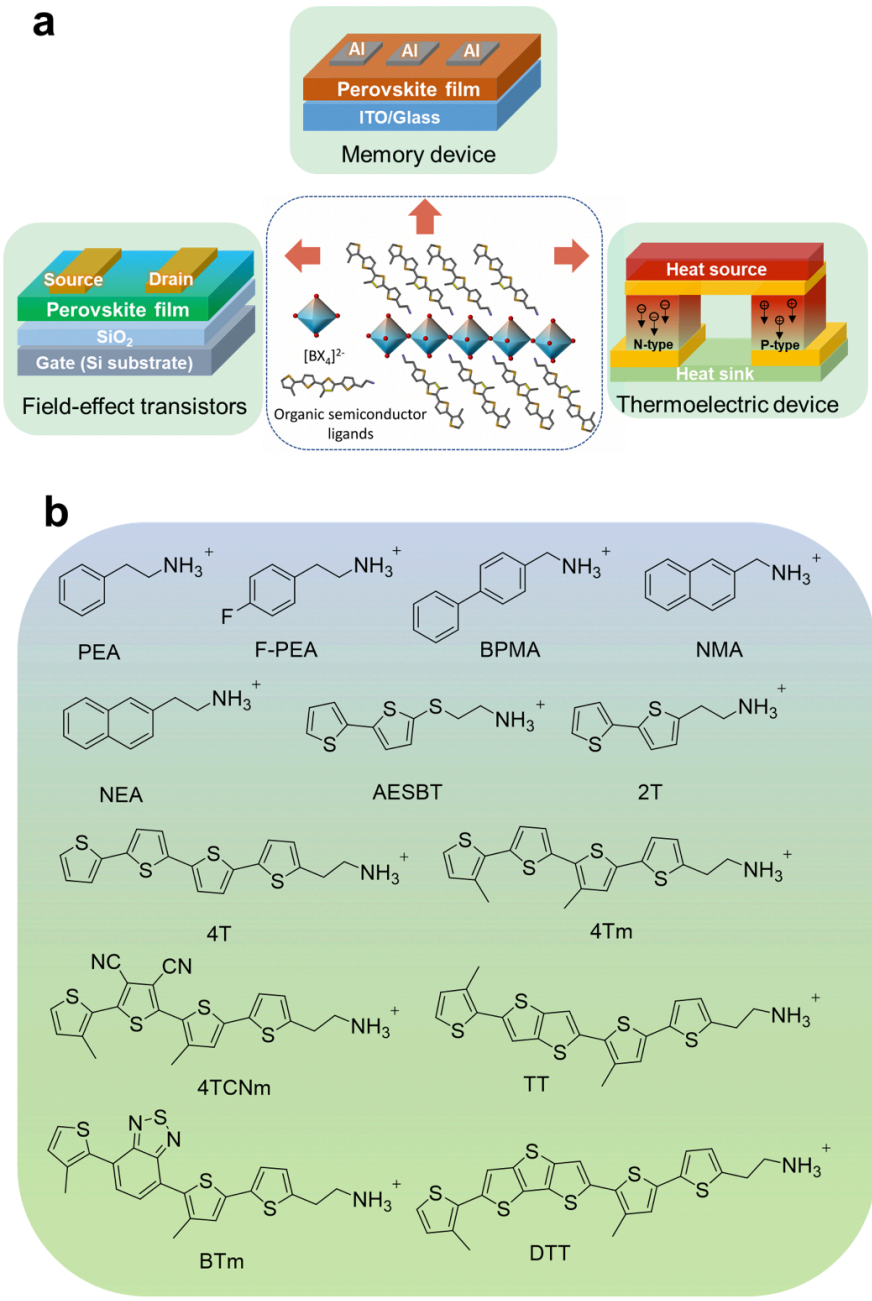

Figure 1. (a) Crystal structures of 2D RP halide perovskites and applications based on halide perovskite materials. (b) Representative conjugated organic ligands for 2D halide perovskites.

3. DEVICE APPLICATIONS

3.1 Perovskite FETs. The first perovskite FET was based on 2D tin-based layered perovskite $(PEA)_2SnI_4$ and reported in 1999.[32] Since then, the progress of perovskite FETs has been relatively

slow compared with perovskite solar cells and light-emitting diodes.[6, 33] For lead-based perovskite FETs, the first bottom gate-top contact (BG-TC) FETs were based on $MAPbI_3$ films as the channel layer, and the device exhibited a hole mobility of 10^{-5} cm^2 V^{-1} s^{-1} at room temperature.[34] However, ion migration and accumulation at the interface hindered the performance and stability of the 3D perovskite FETs. This was proven by operating the device at 78 K where ion migration was mostly suppressed, resulting in reduced hysteresis and improved hole mobility of 2.1×10^{-2} cm^2 V^{-1} s^{-1}.[35] In addition to ion migration, interfacial defects, and inefficient carrier injection have hampered the development of high-performance perovskites FETs.[33] Therefore, sophisticated device engineering and material design are especially important to resolve these challenges, and 2D perovskites are a promising solution.

Compared to 3D perovskites, 2D tin-based perovskite FETs have the advantage of intrinsically suppressing ion migration due to their layered structure.[13, 32, 36, 37] That may be the reason why the first perovskite FET was based on $(PEA)_2SnI_4$ rather than any 3D perovskite.[32] Here, the first BG-TC perovskite FET was fabricated, and it exhibited a hole mobility of ~0.6 cm^2 V^{-1} s^{-1} and a high ON/OFF current ratio of 10^4 at room temperature. Due to this initial success, many FET efforts focused on optimizing the $(PEA)_2SnI_4$ FETs. For example, a high-performance $(PEA)_2SnI_4$ FET with a hole mobility of 15 cm^2 V^{-1} s^{-1}, a high ON/OFF current ratio of 10^6, and a low subthreshold swing (SS) of 0.8 V per decade at room temperature was achieved by a series of optimization processes. These optimization procedures included adding a self-assembled monolayer (SAM)-treated substrate that improves the perovskite morphology, and a MoO_x layer as the hole-injection layer between the perovskite and gold contacts (**Figure 2a**).[36] Notably, other strategies, such as passivating the grain boundaries by adding excess PEA iodide, controlling the crystallization process by applying the Lewis acid-base adduct, and passivating the iodide vacancy

using the oxygen treatment, were also applied (**Figure 2b and 2c**).[37] These results suggest that grain boundary passivation and increasing the grain size are effective strategies to improve FET performance. **Table 1** concludes the important parameters of 2D perovskite FETs.

Table 1. Performance of the 2D perovskites-based FETs.

Perovskites	Structure	Dielectric layer	Treatment	μ_h ($cm^2 V^{-1} s^{-1}$)	I_{on}/I_{off}	SS (V/dec)	Ref
$(PEA)_2SnI_4$	BG-BC	SiO_2	without optimization	0.6	10^4-10^6	/	[32]
$(PEA)_2SnI_4$	BG-BC	SiO_2	Melt processed	2.6	~10^6	/	[38]
$(PEA)_2SnI_4$	TG-TC	Cytop	MoO_x, NH_3I-SAM	15	~10^6	0.8±0.1	[36]
$(PEA)_2SnI_4$	BG-TC	SiO_2	Solvents and precursor	3.5	3.4×10^6	0.8±0.1	[37]
$(4\text{-}FPEA)_2SnI_4$	BG-BC	SiO_2	without optimization	0.48	~10^5	/	[39]
$(DTT)_2SnI_4$	BG-TC	SiO_2	Annealing temperature	0.01	10^3-10^4	~15	[15]
$(4Tm)_2SnI_4$	BG-TC	SiO_2	Annealing temperature	2.32	10^5-10^6	~10	[13]
$(TT)_2SnI_4$	BG-TC	SiO_2	Grain size	9.35	10^5-10^6	~5.4	[15]

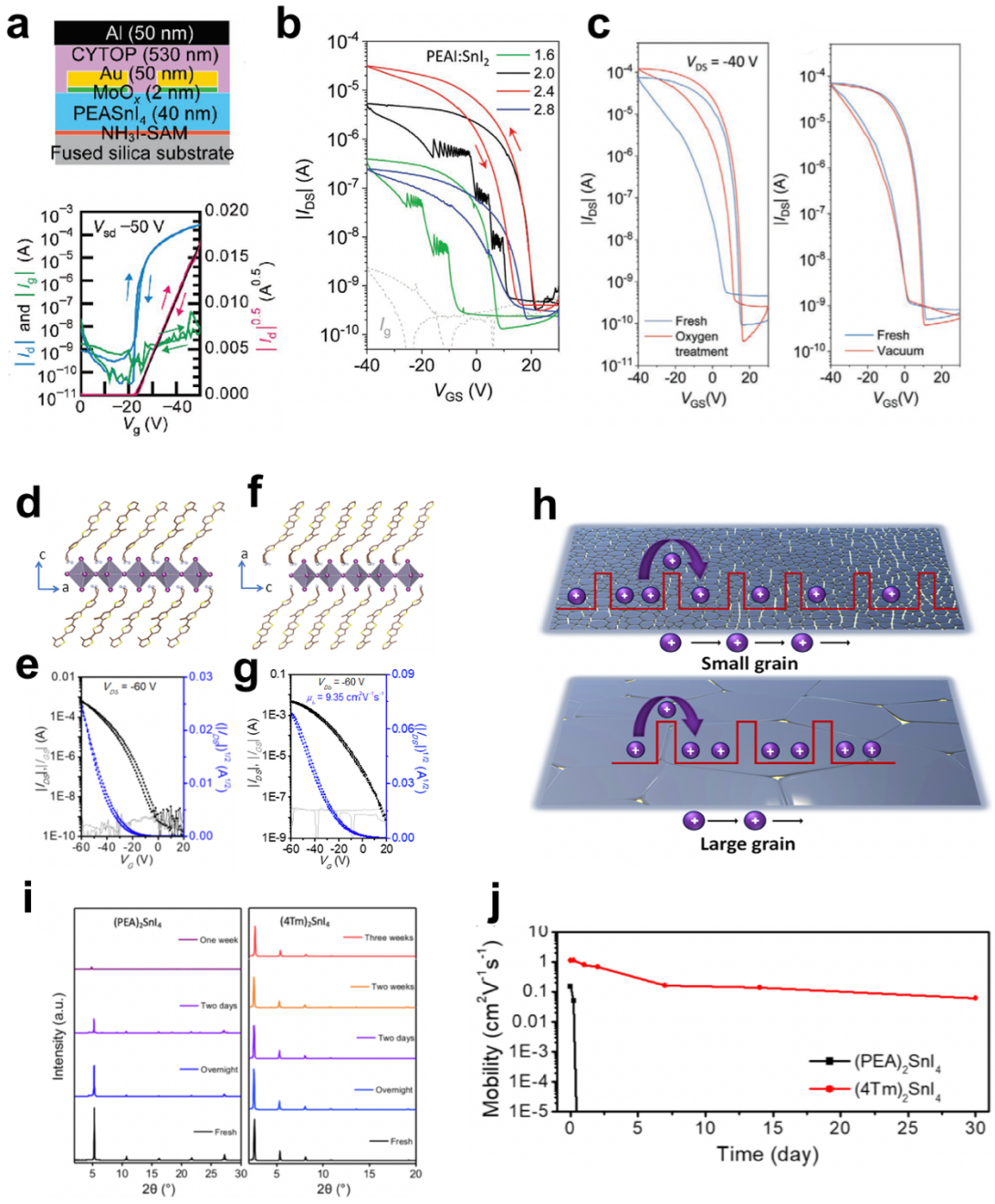

Figure 2. (a) The structure of the $(PEA)_2SnI_4$ FET with SAM-treated substrate and MoO_x hole injection layer and the corresponding transfer characteristics. Image (a) is reproduced with permission from ref. 36. Copyright 2016 [John Wiley and Sons]. The transfer characteristics of FETs based $(PEA)_2SnI_4$ with a series of optimization methods, (b) adding slightly excess PEAI and (c) trace oxygen doping the perovskite film Image (b), (c) are reproduced with permission from ref. 37. Copyright 2020 [John Wiley and Sons]. (d) Side view of the $(4Tm)_2SnI_4$ crystal structures and (e) the corresponding transfer characteristics. (f) Side view of the $(TT)_2SnI_4$ crystal structures and (g) the corresponding transfer characteristics. (h) Illustrations of carrier transport in small-grain and large-grain-based $(TT)_2SnI_4$ thin film. Image (d), (f), (g), (h) are reproduced with permission from ref. 15. Copyright 2021 [American Chemical Society]. (i) Evolution of XRD

patterns of $(PEA)_2SnI_4$ and $(4Tm)_2SnI_4$ films in air. (j) Performance evolution of the $(PEA)_2SnI_4$ and $(4Tm)_2SnI_4$ FETs over long storage time. Image (e), (i), (j) are reproduced with permission from ref. 13. Copyright 2019 [American Chemical Society].

While high-performance $(PEA)_2SnI_4$ FETs can be obtained by intricate device engineering, efforts in developing better active materials were lacking. Inspired by organic semiconductors such as polythiophene, we developed a series of thiophene-based π-conjugated ligands to improve the charge transfer across organic layers, and the oligothiophene ligands were successfully incorporated into 2D perovskite lattices. By modulating the highest occupied molecular orbital (HOMO) and lowest unoccupied molecular orbital (LUMO) energy levels of the ligands, the quantum well structures of OSiP were modified, and in turn, this altered the charge injection properties.[13, 14] Among those conjugated organic cations, the quaterthiophene-based ligand, 2-(3″,4′-dimethyl-[2,2′:5′,2′:5″,2″-quaterthiophen]-5-yl)ethan-1-ammonium (4Tm), was chosen (**Figure 2d**) because 4Tm ligand has a suitable HOMO level that enhances charge injection for n = 1 Sn-based 2D perovskite, as well as its superior stability originated from the higher hydrophobicity.[13] Specifically, the perovskite FET based on $(4Tm)_2SnI_4$ exhibited a higher hole mobility of 2.32 $cm^2 V^{-1} s^{-1}$ (**Figure 2e**) than the perovskite FET based on $(PEA)_2SnI_4$ without any extra treatment, indicating the superiority of $(4Tm)_2SnI_4$. We consider that the improvements were partially attributed to the improved charge injection, which plays a significant role in solution-processed FETs. While conventional ligands (e.g., BA and PEA) suffer from poor charge injection, and thus FET devices have high contact resistance[40], the HOMO of 4Tm matches the work function of Au. This allows for the formation of a suitable contact for hole injection. In addition, incorporating the 4Tm ligand increases the grain size to > 1 μm, which possibly reduces charge scattering at grain boundaries. This hypothesis was further solidified by a novel ligand we recently reported, which is a thienothiophene derivative cation, namely 2-(4'-methyl-5'-(5-(3-

methylthiophen-2-yl)thieno[3,2-b]thiophen-2-yl)-[2,2'-bithiophen]-5-yl)ethan-1-ammonium(TT).[15] Due to the extended π-conjugation and increased planarity, the TT ligand slowed the nucleation process substantially, which led to almost 1 mm-scale grain in the film (**Figure 2f and 2h**). With the extremely large grains, the champion device of $(TT)_2SnI_4$ showed a hole mobility of 9.35 $cm^2\ V^{-1}\ s^{-1}$ and ON/OFF current ratios of $\sim 10^6$ (**Figure 2g**). These improvements were backed by the temperature-dependent transport measurements on devices with different grain sizes. The charge carriers have to overcome more grain boundary potential barriers when the grain sizes are smaller. In addition, the smaller grain size device exhibited higher defect density.

The stability and reproducibility of perovskite FETs is another important parameter for practical applications. Stability can be categorized into operational stability and environmental stability. For Sn-based perovskites, environmental stability is a great challenge because of the easy oxidation of Sn^{2+} to Sn^{4+}. To address this issue, one method is to use Pb-based perovskite instead of Sn-based systems. Recently, a solvent engineering method was applied to process the $MAPbI_3$ film in ambient air, and this allowed researchers to achieve stable ambient air operation of methylammonium lead iodide ($MAPbI_3$) FETs for 120 days.[38] Another way is to suppress the Sn^{2+} oxidation by adding a tin powder into the precursor solution.[37, 41] These engineering methods are effective, while OSiPs have better intrinsic stability that does not require these complicated processing procedures.[13] **Figure 2i** shows the X-ray diffraction (XRD) evolution of $(PEA)_2SnI_4$ and $(4Tm)_2SnI_4$ thin film when stored in air. The diffraction peaks of $(PEA)_2SnI_4$ disappeared after one week. On the contrary, $(4Tm)_2SnI_4$ exhibited similar diffraction peaks over three weeks in air, proving its excellent environmental stability. Similarly, the performance of the $(PEA)_2SnI_4$ device quickly dropped after one day of storage in a glovebox while $(4Tm)_2SnI_4$-based device still

exhibited high mobility after 30 days in air (**Figure 2j**). This improved stability was attributed to the π-conjugated 4Tm molecule being bulkier and more hydrophobic, which in turn, hindered moisture degradation of the inorganic layers. When changing the conjugated organic cations from 4Tm to TT, the $(TT)_2SnI_4$ perovskite also exhibited excellent stability and reproducibility. Specifically, uniform, wafer-scale $(TT)_2SnI_4$ thin films were fabricated, and the mobility of 100 FETs placed upon the wafer achieved an average of 5.35 ± 0.79 $cm^2\ V^{-1}\ s^{-1}$, showcasing the excellent reproducibility of the processing method. More importantly, the $(TT)_2SnI_4$ perovskite FET exhibited excellent operational stability, and the transfer curves were almost unchanged after 1000 time scans.[15] These studies demonstrated why OSiPs are superior than conventional 2D perovskites that provide a new window to achieve highly stable perovskite electronics.

3.2 THERMOELECTRIC DEVICES. Thermoelectric devices are solid-state devices that interconvert heat and electricity, and their efficiency is largely determined by the material figure-of-merit: $ZT = S^2\sigma T/\kappa$. Here, S, σ, T, κ are Seebeck coefficient, electrical conductivity, absolute temperature, and thermal conductivity, respectively. Research interest in employing halide perovskites as thermoelectric materials has grown recently due to the electron-crystal phonon-glass nature (i.e., the materials being good electrical conductors while having poor thermal conductivities).[7, 42-46] Due to the tradeoff between σ and S, tuning the doping levels to an optimal point is of great importance. However, electrical doping of Pb-based perovskites is considered challenging due to the ionic compensation of defects, usually resulting in low carrier concentrations.[26] On the other hand, Sn-based perovskites are more promising due to the spontaneous p-doping caused by the Sn vacancies induced by the oxidation of Sn^{2+} into Sn^{4+} and the interstitial iodine defects.[47-49] Therefore, Sn-based perovskites are more likely to achieve an optimal doping level for thermoelectric applications. For example, Liu et. al. demonstrated the

potential of Sn-based perovskite by making $MASnI_{3-x}Cl_x$ thin films and achieved a value of ZT ~0.14.[50] However, the Sn-based perovskites were unstable in air while the doping level of this work was controlled by air exposure, and over-expose (> 6 minutes) resulted in material degradation. Therefore, 2D perovskite may be a promising replacement to overcome the instability.

Reducing the dimensionality not only improves the stability of halide perovskites but also enhances the performance of the materials in thermoelectric applications in the following manners. First, reducing the dimensionality may increase the power factor ($PF = S^2\sigma$) due to the quantum confinement effect relative to the 3D mother structure with the same Fermi level.[51] This is because the abrupt increase in the density-of-state with respect to energy theoretically allows charge carriers to move heat more efficiently, thus resulting in higher Seebeck coefficient. However, this effect is limited by the quantum well packing density (i.e., the effective channel density). Second, reducing the dimensionality can effectively lower thermal conductivity, a technique that has long been employed for traditional inorganic thermoelectric materials.[52-56] In fact, the thermal conductivity of 2D perovskites can be lowered to ~0.15 W m^{-1} K^{-1}, which is about one-third the value of their 3D counterparts.[57] Lastly, the vertically aligned wells may result in thermionic transport.[58] When transporting across the quantum well structure, the energy barrier resulting from the organic ligands forces the charge carriers to absorb/release more energy, resulting in higher Seebeck coefficient. These factors drive the development of 2D perovskites optimized for TE applications.

Recently, we demonstrated the TE performance of n = 2 $(4Tm)_2FASn_2I_7$ thin films and established the PF dependence on carrier concentrations and temperatures.[59] By intentionally adding Sn^{4+} to the precursor solution, we were able to control the carrier concentration from 2×10^{18}

to 1.2×10^{19} cm^{-3}, obtaining a maximum PF of 7.07 μW m^{-1} K^{-2} at 333 K. The thermal conductivity of the material was determined to be 0.126 W m^{-1} K^{-1}, resulting in a ZT ~0.02 at room temperature. The transport property trend of the 2D perovskite agrees well with traditional inorganic semiconductors where the electrical conductivity decreases and Seebeck coefficient increases with temperature, and there is strong tradeoff between the carrier concentration and Seebeck coefficient (**Figure 3a-c**). The resulting thin films also showed robust thermal stability at mild temperature (i.e., at values < 313 K) for over 100 h. Above this temperature, thermal dedoping was observed where the carrier concentration decreased, possibly due to the self-healing characteristic of the 2D perovskites. For non-conjugated ligands, Yang et. al. reported the TE performance of PEA-based 2D perovskites and concluded that the carrier concentration can also be controlled by the n number and MACl doping.[60] With extraordinarily high Seebeck coefficients, a much higher PF of 111 μW m^{-1} K^{-2} was achieved with n = 2 ~ 4 MACl doped $PEA_2MA_{n-1}Sn_nI_{3n+1}$ thin films (**Figure 3d-f**). The authors attributed the high Seebeck coefficient to the quantum confinement effect. However, the PEA-based 2D perovskites are much less stable than 4Tm-based 2D perovskites, and they degrade within several minutes in air. In addition, the Seebeck coefficients of this work were measured in ambient conditions and showed ± 200 μV K^{-1} fluctuations from –30 °C to 30 °C, making the conclusions derived from these variable results somewhat less reliable. This reinforces the idea that it is important to minimize the measurement errors to increase the reliability and accuracy of the TE properties, especially for perovskite-based systems that are known to be susceptible to chemical and structural changes during device operation.

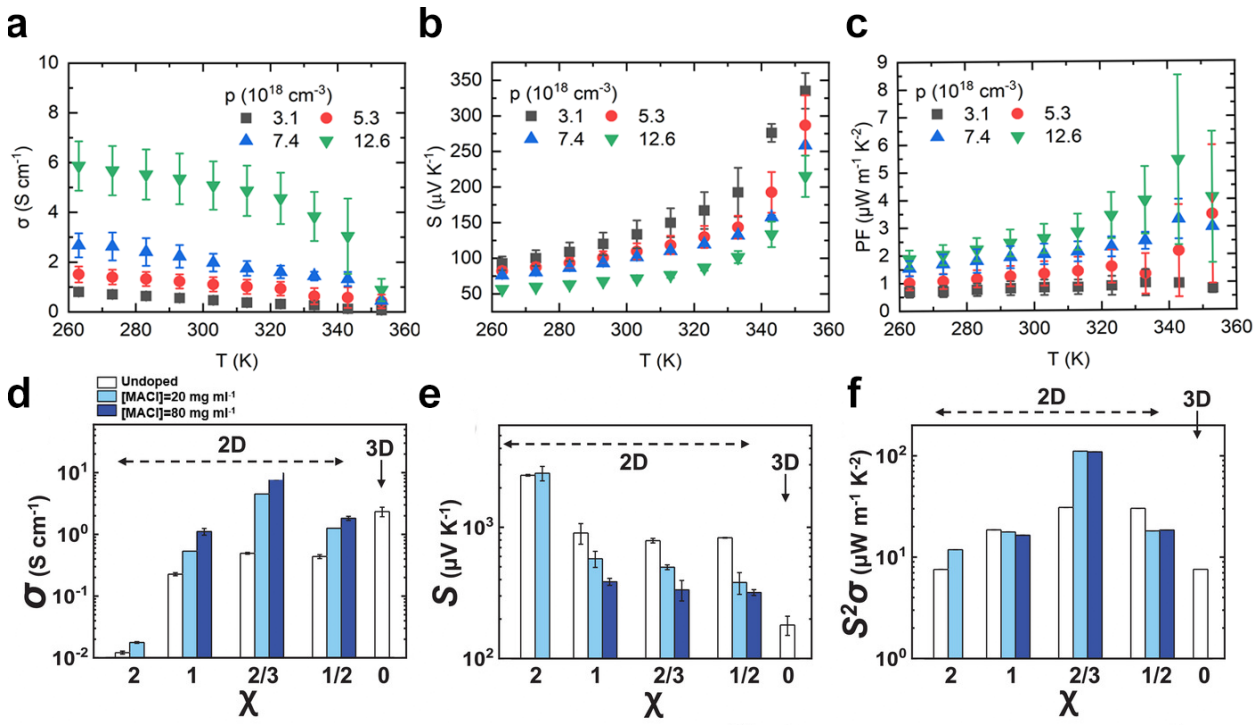

Figure 3. Dependence of the **(a)** electrical conductivity, **(b)** Seebeck coefficient, and **(c)** power factor on average temperatures of the $(4Tm)_2FASn_2I_7$ thin films. Each data point shown was compiled from multiple sets of data whose carrier concentration (p) values are approximately the same, and different symbols represent the thermoelectric performance of different average carrier concentration values. Image (a), (b), (c) are reproduced with permission from ref. 59. Copyright 2021 [American Chemical Society]. Dependence of the **(d)** electrical conductivity, **(e)** Seebeck coefficient, and **(f)** power factor on precursor solution composition of $(PEA)_2MA_{n-1}Sn_nI_{3n+1}$ thin films. ($\chi = 2 \rightarrow n = 1$, $\chi = 1 \rightarrow n = 2$, $\chi = 2/3 \rightarrow n = 3$, $\chi = 1/2 \rightarrow n = 4$, $\chi = 0 \rightarrow$ 3D $MASnI_3$). Image (d), (e), (f) are reproduced with permission from ref. 60. Copyright 2021 [John Wiley and Sons].

The development of 2D perovskites as TE materials is still in the earliest of stages. Overall, the carrier mobility of 2D perovskites certainly can be improved significantly as both of the efforts described above report relatively low hole mobility values. This is because 2D perovskites need to have a high enough n number to allow higher carrier concentration for optimal power factor, yet achieving phase purity in $n > 1$ 2D perovskite is not trivial. Phase impurities can lead to extra electron scattering due to the mismatch of band edges between phases, which is detrimental to carrier mobility. Manipulating the phase distribution of 2D perovskites can certainly help in achieving this goal.[61-64] On the other hand, the reduction of thermal conductivity due to the 2D

structure could be compromised at higher n number. As such, it is important to find the optimal n number that manifests the ultralow thermal conductivity nature while enabling high electrical conductivity and Seebeck coefficient. Finally, consistent effort is required on efficient electrical doping of halide perovskites for the innate instability of defects in halide perovskites and the easily altered doping level due to air exposure. From this perspective, conjugated ligands like 4Tm have an edge in turns of overall stability and we expect the thermoelectric performance of 2D perovskites incorporating semiconducting ligands continue to grow.

3.3 PEROVSKITE MEMORY. Hysteresis is a well-known phenomenon in halide perovskites-based devices where forward and reverse I-V scans do not overlap. Hysteresis within halide perovskites is attributed to one of many possible factors, including ion migration and interfacial defects. While hysteresis is usually undesirable for devices such as solar cells, LEDs, and FETs, it may actually be an advantage for memory applications. Therefore, nonvolatile resistive switching memory (RSM) based on halide perovskite is another emerging research field that has been considered due to their low operation voltages and high ON/OFF ratios.[65] Recently, perovskite memory devices were evaluated using a high-throughput screening method based on first-principles calculations and select dimer-$Cs_3Sb_2I_9$ for fabricating memory (**Figure 4a**).[66] A memory device-based dimer-$Cs_3Sb_2I_9$ has an ultra-fast switching speed (~20 ns), exhibited excellent retention properties, and the low-resistance state (LRS) and high-resistance state (HRS) remained stable for 5000 s without degradation (**Figure 4b**). The work shows the feasibility of designing perovskite-based memory with ultra-fast switching speed and well retention properties. The perovskite memory device was fabricated by combining first-principles screening and experimental techniques. Based on the calculation results, two types of perovskite were synthesized, $CsPb_2Br_5$ and $CsPbBr_3$ as resistive switching layers to fabricate the perovskite

memory, and the perovskite memory exhibits high environmental stability and low operating voltage (**Figure 4c**).[67] **Figure 4d** shows that $CsPb_2Br_5$ and $CsPbBr_3$-based memory have retention properties under a reading voltage of 0.1 V. Despite these progresses, it is still necessary to further improve the stability of memory devices to over 10 years to compete with current commercially-available technologies.[68]

Among these memory device structures, transistor memory devices have been of great interest due to the advantage of nondestructive readout and high memory performance. Recently, a transistor memory with $(PEA)_2PbBr_4$ active layer was achieved by adding the organic semiconductor 2,7-dioctyl[1]benzothieno[3,2-b]benzothiophene (C8-BTBT) into the perovskite precursor solution (**Figure 4e**).[69] The resulting transistor memory exhibited a memory window (>180 V) (**Figure 4f**), a high erase/write channel current ratio (10^4), good data retention (**Figure 4g**), and high endurance (>10^4 cycles). In this device, the C8-BTBT-rich phase acted as the hole-transporting channel while the $(PEA)_2PbBr_4$ acted as the charge storage element. This transistor memory exhibited hole mobility of 5×10^{-2} cm^2 V^{-1} s^{-1}, which is rather low. To improve the performance of 2D perovskite transistor memory, we propose adopting OSiPs as the active layer materials. Using OSiPs not only brings about excellent stability, but also increases the charge carrier mobility of the materials. As OSiPs actively participate in the charge transport process, not just as charge storage sites, achieving high mobility while having good memory performance may be challenging. As such, identifying effective strategies towards both enhanced FET mobility and better memory performance in the devices is an important future direction.

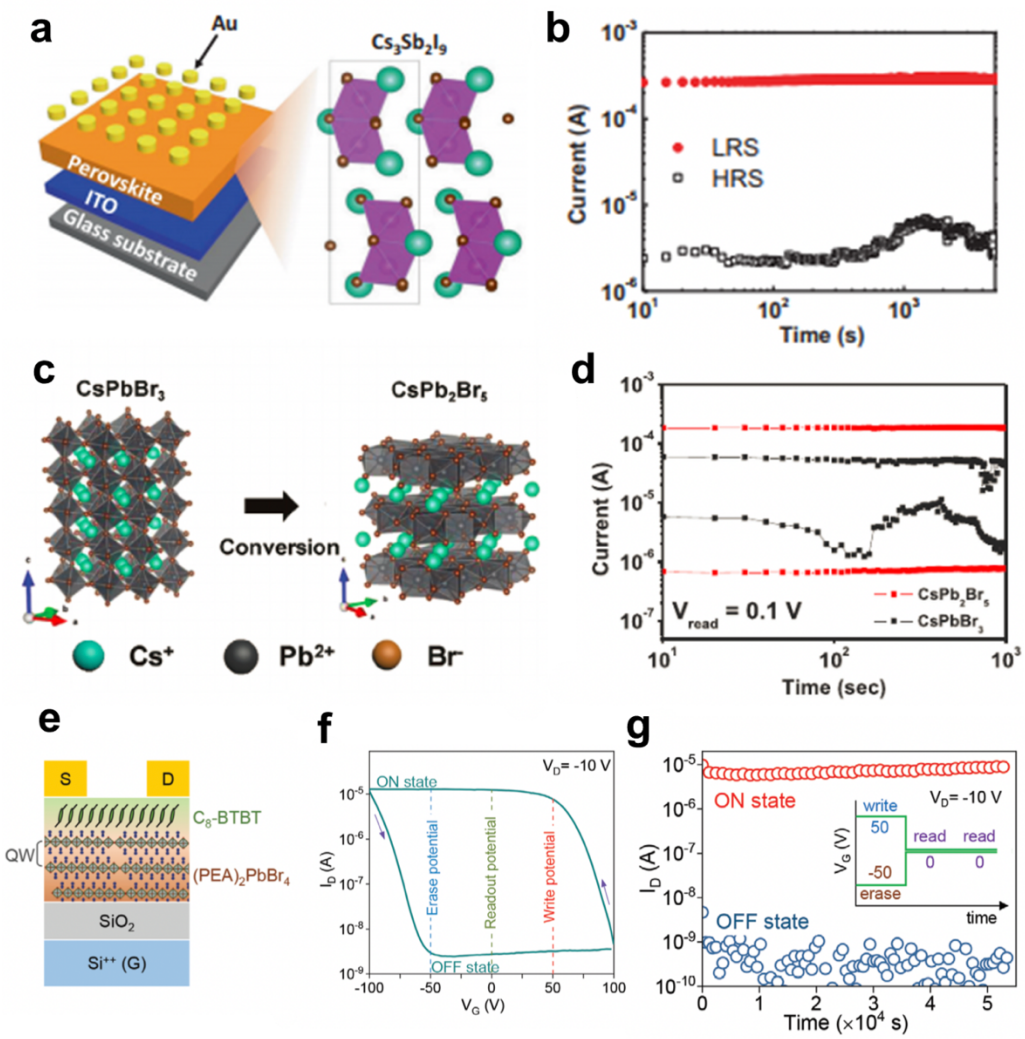

Figure 4. **(a)** Schematic illustration of RSM device and **(b)** data retention properties of the dimer-$Cs_3Sb_2I_9$. Image (a), (b) are reproduced with permission from ref. 66. Copyright 2021 [Springer Nature]. **(c)** Phase transformation from $CsPbBr_3$ to $CsPb_2Br_5$. **(d)** Data retention properties of Au/$CsPbBr_3$/ITO and Au/ $CsPb_2Br_5$/ITO. Image (c), (d) are reproduced with permission from ref. 67. Copyright 2021 [John Wiley and Sons]. **(e)** Schematic of a transistor, **(f)** representative transistor transfer curve, and **(g)** memory retention characteristics of based $(PEA)_2PbBr_4$ and C8-BTBT. Image (e), (f), (g) are reproduced with permission from ref. 69. Copyright 2021 [John Wiley and Sons].

4. CONCLUSIONS AND OUTLOOK

In summary, OSiPs are next-generation semiconductors that successfully solve the charge injection issues of 2D perovskite while improving the materials' intrinsic stability. OSiPs have tremendous potential in different optoelectronic (e.g., solar cells and LEDs) and electronic (e.g.,

FET, thermoelectric devices, and memory devices) applications. More importantly, there are still many applications that 2D OSiPs could explore, such as X-ray detectors, photo-transistors, and optically pumped and switched devices. In this way, OSiPs can be instrumental in realizing higher performing devices while providing a pathway to understand the interactions between organic and inorganic layers. Furthermore, more exciting functional ligands that fit better with their end-use purpose can be realized by following the design concept of OSiPs. For example, extending the thiophene unit in the conjugated backbone, optimizing the structure of the material by adopting heteroatoms (O, S, and Se), and changing the number of fluorine atoms are all possible means to enhance the functionality of the ligands.

Despite OSiPs have excellent electronic properties, it remains a great challenge to develop the full palette of perovskite structure-property relationships. For instance, organic semiconductor ligands have a wide chemical space for materials design, which provides a possibility of introducing a wide variety of functional organic building blocks incorporated into the inorganic lattice. Currently, research on OSiPs is limited to 2D perovskites with low n values. Because higher n 2D perovskites could have higher mobility, it is definitely necessary to explore these materials in FET, thermoelectric devices, and transistor memories. Yet the ion migration exists in high value of perovskite materials and still has an issue in performance and stability of devices, how to hinder the ion migration is very important. Furthermore, obtaining phase-pure higher n single crystals and thin films are more challenging and new processing methods are needed. Of course, the rise of machine learning and artificial intelligence protocols may provide a key means to probe structure-property relationships in a high-throughput manner. Then, experimentalists can combine the computational and experimental results to obtain the optimized molecular structure, which can increase the success rate of material design. We believe that with a deeper fundamental

understanding of the relationship between the ligand chemistry, crystal structure, morphology, and electronic properties of the OSiPs, we will be able to improve the performance of OSiPs-based devices.

AUTHOR INFORMATION

Corresponding Author

dou10@purdue.edu

Notes

The authors declare no competing financial interest.

Author Contributions

The manuscript was written through contributions of all authors. All authors have given approval to the final version of the manuscript.

ACKNOWLEDGMENT

The work was supported the National Science Foundation (Award Number: 2110706-DMR, Program Manager: Dr. Paul Lane).

REFERENCES

(1) Kim, J. Y.; Lee, J.-W.; Jung, H. S.; Shin, H.; Park, N.-G. High-Efficiency Perovskite Solar Cells. *Chem. Rev.* **2020**, *120* (15), 7867-7918.
(2) Wang, R.; Huang, T.; Xue, J.; Tong, J.; Zhu, K.; Yang, Y. Prospects for metal halide perovskite-based tandem solar cells. *Nat. Photonics* **2021**, *15* (6), 411-425.
(3) Liu, X.-K.; Xu, W.; Bai, S.; Jin, Y.; Wang, J.; Friend, R. H.; Gao, F. Metal halide perovskites for light-emitting diodes. *Nat. Mater.* **2021**, *20* (1), 10-21.
(4) Chen, S.; Dai, X.; Xu, S.; Jiao, H.; Zhao, L.; Huang, J. Stabilizing perovskite-substrate interfaces for high-performance perovskite modules. *Science* **2021**, *373* (6557), 902-907.
(5) Cao, Y.; Wang, N.; Tian, H.; Guo, J.; Wei, Y.; Chen, H.; Miao, Y.; Zou, W.; Pan, K.; He, Y.; Cao, H.; Ke, Y.; Xu, M.; Wang, Y.; Yang, M.; Du, K.; Fu, Z.; Kong, D.; Dai, D.; Jin,

Y.; Li, G.; Li, H.; Peng, Q.; Wang, J.; Huang, W. Perovskite light-emitting diodes based on spontaneously formed submicrometre-scale structures. *Nature* **2018**, *562* (7726), 249-253.
(6) Liang, Y.; Li, F.; Zheng, R. Low-Dimensional Hybrid Perovskites for Field-Effect Transistors with Improved Stability: Progress and Challenges. *Adv. Electron. Mater.* **2020**, *6* (9), 2000137.
(7) Haque, M. A.; Kee, S.; Villalva, D. R.; Ong, W.-L.; Baran, D. Halide Perovskites: Thermal Transport and Prospects for Thermoelectricity. *Adv. Sci.* **2020**, *7* (10), 1903389.
(8) Di, J.; Du, J.; Lin, Z.; Liu, S.; Ouyang, J.; Chang, J. Recent advances in resistive random access memory based on lead halide perovskite. *InfoMat* **2021**, *3* (3), 293-315.
(9) Dou, L. Emerging two-dimensional halide perovskite nanomaterials. *J.Mater. Chem. C* **2017**, *5* (43), 11165-11173.
(10) Shi, E.; Gao, Y.; Finkenauer, B. P.; Akriti; Coffey, A. H.; Dou, L. Two-dimensional halide perovskite nanomaterials and heterostructures. *Chem. Soc. Rev.* **2018**, *47* (16), 6046-6072.
(11) Park, I.-H.; Chu, L.; Leng, K.; Choy, Y. F.; Liu, W.; Abdelwahab, I.; Zhu, Z.; Ma, Z.; Chen, W.; Xu, Q.-H.; Eda, G.; Loh, K. P. Highly Stable Two-Dimensional Tin(II) Iodide Hybrid Organic–Inorganic Perovskite Based on Stilbene Derivative. *Adv. Funct. Mater.* **2019**, *29* (39), 1904810.
(12) Hu, J.; Oswald, I. W. H.; Stuard, S. J.; Nahid, M. M.; Zhou, N.; Williams, O. F.; Guo, Z.; Yan, L.; Hu, H.; Chen, Z.; Xiao, X.; Lin, Y.; Yang, Z.; Huang, J.; Moran, A. M.; Ade, H.; Neilson, J. R.; You, W. Synthetic control over orientational degeneracy of spacer cations enhances solar cell efficiency in two-dimensional perovskites. *Nat. Commun.* **2019**, *10* (1), 1276.
(13) Gao, Y.; Wei, Z.; Yoo, P.; Shi, E.; Zeller, M.; Zhu, C.; Liao, P.; Dou, L. Highly Stable Lead-Free Perovskite Field-Effect Transistors Incorporating Linear π-Conjugated Organic Ligands. *J. Am. Chem. Soc.* **2019**, *141* (39), 15577-15585.
(14) Gao, Y.; Shi, E.; Deng, S.; Shiring, S. B.; Snaider, J. M.; Liang, C.; Yuan, B.; Song, R.; Janke, S. M.; Liebman-Peláez, A.; Yoo, P.; Zeller, M.; Boudouris, B. W.; Liao, P.; Zhu, C.; Blum, V.; Yu, Y.; Savoie, B. M.; Huang, L.; Dou, L. Molecular engineering of organic–inorganic hybrid perovskites quantum wells. *Nat. Chem.* **2019**, *11* (12), 1151-1157.
(15) Liang, A.; Gao, Y.; Asadpour, R.; Wei, Z.; Finkenauer, B. P.; Jin, L.; Yang, J.; Wang, K.; Chen, K.; Liao, P.; Zhu, C.; Huang, L.; Boudouris, B. W.; Alam, M. A.; Dou, L. Ligand-Driven Grain Engineering of High Mobility Two-Dimensional Perovskite Thin-Film Transistors. *J. Am. Chem. Soc.* **2021**, *143* (37), 15215-15223.
(16) Gao, Y.; Dou, L. Organic semiconductor-incorporated two-dimensional halide perovskites. *Natl. Sci. Rev.* **2021**, DOI: 10.1093/nsr/nwab111.
(17) Leng, K.; Li, R.; Lau, S. P.; Loh, K. P. Ferroelectricity and Rashba effect in 2D organic–inorganic hybrid perovskites. *Trends Chem* **2021**, *3* (9), 716-732.
(18) Jena, A. K.; Kulkarni, A.; Miyasaka, T. Halide Perovskite Photovoltaics: Background, Status, and Future Prospects. *Chem. Rev.* **2019**, *119* (5), 3036-3103.
(19) Zhang, F.; Lu, H.; Tong, J.; Berry, J. J.; Beard, M. C.; Zhu, K. Advances in two-dimensional organic–inorganic hybrid perovskites. *Energy Environ. Sci.* **2020**, *13* (4), 1154-1186.
(20) Quan, L. N.; Yuan, M.; Comin, R.; Voznyy, O.; Beauregard, E. M.; Hoogland, S.; Buin, A.; Kirmani, A. R.; Zhao, K.; Amassian, A.; Kim, D. H.; Sargent, E. H. Ligand-Stabilized Reduced-Dimensionality Perovskites. *J. Am. Chem. Soc.* **2016**, *138* (8), 2649-2655.
(21) Leng, K.; Fu, W.; Liu, Y.; Chhowalla, M.; Loh, K. P. From bulk to molecularly thin hybrid perovskites. *Nat. Rev. Mater.* **2020**, *5* (7), 482-500.

(22) Shi, E.; Yuan, B.; Shiring, S. B.; Gao, Y.; Akriti; Guo, Y.; Su, C.; Lai, M.; Yang, P.; Kong, J.; Savoie, B. M.; Yu, Y.; Dou, L. Two-dimensional halide perovskite lateral epitaxial heterostructures. *Nature* **2020**, *580* (7805), 614-620.
(23) Akriti; Shi, E.; Shiring, S. B.; Yang, J.; Atencio-Martinez, C. L.; Yuan, B.; Hu, X.; Gao, Y.; Finkenauer, B. P.; Pistone, A. J.; Yu, Y.; Liao, P.; Savoie, B. M.; Dou, L. Layer-by-layer anionic diffusion in two-dimensional halide perovskite vertical heterostructures. *Nat. Nanotechnol.* **2021**, *16* (5), 584-591.
(24) Li, X.; Hoffman, J. M.; Kanatzidis, M. G. The 2D Halide Perovskite Rulebook: How the Spacer Influences Everything from the Structure to Optoelectronic Device Efficiency. *Chem. Rev.* **2021**, *121* (4), 2230-2291.
(25) Mao, L.; Stoumpos, C. C.; Kanatzidis, M. G. Two-Dimensional Hybrid Halide Perovskites: Principles and Promises. *J. Am. Chem. Soc.* **2019**, *141* (3), 1171-1190.
(26) Euvrard, J.; Yan, Y.; Mitzi, D. B. Electrical doping in halide perovskites. *Nat. Rev. Mater.* **2021**, *6* (6), 531-549.
(27) Blancon, J.-C.; Even, J.; Stoumpos, C. C.; Kanatzidis, M. G.; Mohite, A. D. Semiconductor physics of organic–inorganic 2D halide perovskites. *Nat. Nanotechnol.* **2020**, *15* (12), 969-985.
(28) Calabrese, J.; Jones, N. L.; Harlow, R. L.; Herron, N.; Thorn, D. L.; Wang, Y. Preparation and characterization of layered lead halide compounds. *J. Am. Chem. Soc.* **1991**, *113* (6), 2328-2330.
(29) Hu, H.; Zhao, D.; Gao, Y.; Qiao, X.; Salim, T.; Chen, B.; Chia, E. E. M.; Grimsdale, A. C.; Lam, Y. M. Harvesting Triplet Excitons in Lead-Halide Perovskites for Room-Temperature Phosphorescence. *Chem. Mater.* **2019**, *31* (7), 2597-2602.
(30) Du, K.-z.; Tu, Q.; Zhang, X.; Han, Q.; Liu, J.; Zauscher, S.; Mitzi, D. B. Two-Dimensional Lead(II) Halide-Based Hybrid Perovskites Templated by Acene Alkylamines: Crystal Structures, Optical Properties, and Piezoelectricity. *Inorg. Chem.* **2017**, *56* (15), 9291-9302.
(31) Zhu, X.-H.; Mercier, N.; Frère, P.; Blanchard, P.; Roncali, J.; Allain, M.; Pasquier, C.; Riou, A. Effect of Mono- versus Di-ammonium Cation of 2,2'-Bithiophene Derivatives on the Structure of Organic−Inorganic Hybrid Materials Based on Iodo Metallates. *Inorg. Chem.* **2003**, *42* (17), 5330-5339.
(32) Kagan, C. R.; Mitzi, D. B.; Dimitrakopoulos, C. D. Organic-Inorganic Hybrid Materials as Semiconducting Channels in Thin-Film Field-Effect Transistors. *Science* **1999**, *286* (5441), 945-947.
(33) Paulus, F.; Tyznik, C.; Jurchescu, O. D.; Vaynzof, Y. Switched-On: Progress, Challenges, and Opportunities in Metal Halide Perovskite Transistors. *Adv. Funct. Mater.* **2021**, *31* (29), 2101029.
(34) Heo, J. H.; Im, S. H.; Noh, J. H.; Mandal, T. N.; Lim, C.-S.; Chang, J. A.; Lee, Y. H.; Kim, H.-j.; Sarkar, A.; Nazeeruddin, M. K.; Grätzel, M.; Seok, S. I. Efficient inorganic–organic hybrid heterojunction solar cells containing perovskite compound and polymeric hole conductors. *Nat. Photonics* **2013**, *7* (6), 486-491.
(35) Chin, X. Y.; Cortecchia, D.; Yin, J.; Bruno, A.; Soci, C. Lead iodide perovskite light-emitting field-effect transistor. *Nat. Commun.* **2015**, *6* (1), 7383.
(36) Matsushima, T.; Hwang, S.; Sandanayaka, A. S. D.; Qin, C.; Terakawa, S.; Fujihara, T.; Yahiro, M.; Adachi, C. Solution-Processed Organic–Inorganic Perovskite Field-Effect Transistors with High Hole Mobilities. *Adv. Mater.* **2016**, *28* (46), 10275-10281.
(37) Zhu, H.; Liu, A.; Shim, K. I.; Hong, J.; Han, J. W.; Noh, Y.-Y. High-Performance and Reliable Lead-Free Layered-Perovskite Transistors. *Adv. Mater.* **2020**, *32* (31), 2002717.

(38) Mativenga, M.; Ji, J.; Hoang, N. T. t.; Haque, F. Ambient Air Stability of Hybrid Perovskite Thin-Film Transistors by Ambient Air Processing. *Adv. Mater. Interfaces* **2020**, *7* (6), 1901777.
(39) Mitzi, D. B.; Dimitrakopoulos, C. D.; Kosbar, L. L. Structurally Tailored Organic–Inorganic Perovskites: Optical Properties and Solution-Processed Channel Materials for Thin-Film Transistors. *Chem. Mater.* **2001**, *13* (10), 3728-3740.
(40) Li, M.-K.; Chen, T.-P.; Lin, Y.-F.; Raghavan, C. M.; Chen, W.-L.; Yang, S.-H.; Sankar, R.; Luo, C.-W.; Chang, Y.-M.; Chen, C.-W. Intrinsic Carrier Transport of Phase-Pure Homologous 2D Organolead Halide Hybrid Perovskite Single Crystals. *Small* **2018**, *14* (52), 1803763.
(41) Lin, R.; Xiao, K.; Qin, Z.; Han, Q.; Zhang, C.; Wei, M.; Saidaminov, M. I.; Gao, Y.; Xu, J.; Xiao, M.; Li, A.; Zhu, J.; Sargent, E. H.; Tan, H. Monolithic all-perovskite tandem solar cells with 24.8% efficiency exploiting comproportionation to suppress Sn(ii) oxidation in precursor ink. *Nat. Energy* **2019**, *4* (10), 864-873.
(42) He, Y.; Galli, G. Perovskites for Solar Thermoelectric Applications: A First Principle Study of CH3NH3AI3 (A = Pb and Sn). *Chem. Mater.* **2014**, *26* (18), 5394-5400.
(43) Filippetti, A.; Caddeo, C.; Delugas, P.; Mattoni, A. Appealing Perspectives of Hybrid Lead–Iodide Perovskites as Thermoelectric Materials. *J. Phys. Chem. C* **2016**, *120* (50), 28472-28479.
(44) Ye, T.; Wang, X.; Li, X.; Yan, A. Q.; Ramakrishna, S.; Xu, J. Ultra-high Seebeck coefficient and low thermal conductivity of a centimeter-sized perovskite single crystal acquired by a modified fast growth method. *J.Mater. Chem. C* **2017**, *5* (5), 1255-1260.
(45) Miyata, K.; Atallah, T. L.; Zhu, X.-Y. Lead halide perovskites: Crystal-liquid duality, phonon glass electron crystals, and large polaron formation. *Sci. Adv.* **2017**, *3* (10), e1701469.
(46) Xie, H.; Hao, S.; Bao, J.; Slade, T. J.; Snyder, G. J.; Wolverton, C.; Kanatzidis, M. G. All-Inorganic Halide Perovskites as Potential Thermoelectric Materials: Dynamic Cation off-Centering Induces Ultralow Thermal Conductivity. *J. Am. Chem. Soc.* **2020**, *142* (20), 9553-9563.
(47) Meggiolaro, D.; Ricciarelli, D.; Alasmari, A. A.; Alasmary, F. A. S.; De Angelis, F. Tin versus Lead Redox Chemistry Modulates Charge Trapping and Self-Doping in Tin/Lead Iodide Perovskites. *J. Phys. Chem. Lett.* **2020**, *11* (9), 3546-3556.
(48) Takahashi, Y.; Hasegawa, H.; Takahashi, Y.; Inabe, T. Hall mobility in tin iodide perovskite CH3NH3SnI3: Evidence for a doped semiconductor. *J. Solid State Chem.* **2013**, *205* 39-43.
(49) Takahashi, Y.; Obara, R.; Lin, Z.-Z.; Takahashi, Y.; Naito, T.; Inabe, T.; Ishibashi, S.; Terakura, K. Charge-transport in tin-iodide perovskite CH3NH3SnI3: origin of high conductivity. *Dalton Trans.* **2011**, *40* (20), 5563-5568.
(50) Liu, T.; Zhao, X.; Li, J.; Liu, Z.; Liscio, F.; Milita, S.; Schroeder, B. C.; Fenwick, O. Enhanced control of self-doping in halide perovskites for improved thermoelectric performance. *Nat. Commun.* **2019**, *10* (1), 5750.
(51) Kim, R.; Datta, S.; Lundstrom, M. S. Influence of dimensionality on thermoelectric device performance. *J. Appl. Phys.* **2009**, *105* (3), 034506.
(52) Dresselhaus, M. S.; Chen, G.; Tang, M. Y.; Yang, R. G.; Lee, H.; Wang, D. Z.; Ren, Z. F.; Fleurial, J.-P.; Gogna, P. New Directions for Low-Dimensional Thermoelectric Materials. *Adv. Mater.* **2007**, *19* (8), 1043-1053.
(53) Venkatasubramanian, R.; Siivola, E.; Colpitts, T.; O'Quinn, B. Thin-film thermoelectric devices with high room-temperature figures of merit. *Nature* **2001**, *413* (6856), 597-602.
(54) Harman, T. C.; Taylor, P. J.; Walsh, M. P.; LaForge, B. E. Quantum Dot Superlattice Thermoelectric Materials and Devices. *Science* **2002**, *297* (5590), 2229-2232.

(55) Caylor, J. C.; Coonley, K.; Stuart, J.; Colpitts, T.; Venkatasubramanian, R. Enhanced thermoelectric performance in PbTe-based superlattice structures from reduction of lattice thermal conductivity. *Appl. Phys. Lett.* **2005**, *87* (2), 023105.
(56) Hicks, L. D.; Dresselhaus, M. S. Effect of quantum-well structures on the thermoelectric figure of merit. *Phys. Rev. B* **1993**, *47* (19), 12727-12731.
(57) Giri, A.; Chen, A. Z.; Mattoni, A.; Aryana, K.; Zhang, D.; Hu, X.; Lee, S.-H.; Choi, J. J.; Hopkins, P. E. Ultralow Thermal Conductivity of Two-Dimensional Metal Halide Perovskites. *Nano Lett.* **2020**, *20* (5), 3331-3337.
(58) Zide, J. M. O.; Vashaee, D.; Bian, Z. X.; Zeng, G.; Bowers, J. E.; Shakouri, A.; Gossard, A. C. Demonstration of electron filtering to increase the Seebeck coefficient in $In_{0.53}Ga_{0.47}As/In_{0.53}Ga_{0.28}Al_{0.19}As$ superlattices. *Phys. Rev. B* **2006**, *74* (20), 205335.
(59) Hsu, S.-N.; Zhao, W.; Gao, Y.; Akriti; Segovia, M.; Xu, X.; Boudouris, B. W.; Dou, L. Thermoelectric Performance of Lead-Free Two-Dimensional Halide Perovskites Featuring Conjugated Ligands. *Nano Lett.* **2021**, *21* (18), 7839-7844.
(60) Yang, S. J.; Kim, D.; Choi, J.; Kim, S. H.; Park, K.; Ryu, S.; Cho, K. Enhancing Thermoelectric Power Factor of 2D Organometal Halide Perovskites by Suppressing 2D/3D Phase Separation. *Adv. Mater.* **2021**, *33* (38), 2102797.
(61) Xing, J.; Zhao, Y.; Askerka, M.; Quan, L. N.; Gong, X.; Zhao, W.; Zhao, J.; Tan, H.; Long, G.; Gao, L.; Yang, Z.; Voznyy, O.; Tang, J.; Lu, Z.-H.; Xiong, Q.; Sargent, E. H. Color-stable highly luminescent sky-blue perovskite light-emitting diodes. *Nat. Commun.* **2018**, *9* (1), 3541.
(62) Wang, C.; Han, D.; Wang, J.; Yang, Y.; Liu, X.; Huang, S.; Zhang, X.; Chang, S.; Wu, K.; Zhong, H. Dimension control of in situ fabricated CsPbClBr2 nanocrystal films toward efficient blue light-emitting diodes. *Nat. Commun.* **2020**, *11* (1), 6428.
(63) Meng, F.; Liu, X.; Chen, Y.; Cai, X.; Li, M.; Shi, T.; Chen, Z.; Chen, D.; Yip, H.-L.; Ramanan, C.; Blom, P. W. M.; Su, S.-J. Co-Interlayer Engineering toward Efficient Green Quasi-Two-Dimensional Perovskite Light-Emitting Diodes. *Adv. Funct. Mater.* **2020**, *30* (19), 1910167.
(64) Sun, C.; Jiang, Y.; Cui, M.; Qiao, L.; Wei, J.; Huang, Y.; Zhang, L.; He, T.; Li, S.; Hsu, H.-Y.; Qin, C.; Long, R.; Yuan, M. High-performance large-area quasi-2D perovskite light-emitting diodes. *Nat. Commun.* **2021**, *12* (1), 2207.
(65) Li, B.; Hui, W.; Ran, X.; Xia, Y.; Xia, F.; Chao, L.; Chen, Y.; Huang, W. Metal halide perovskites for resistive switching memory devices and artificial synapses. *J.Mater. Chem. C* **2019**, *7* (25), 7476-7493.
(66) Park, Y.; Kim, S. H.; Lee, D.; Lee, J.-S. Designing zero-dimensional dimer-type all-inorganic perovskites for ultra-fast switching memory. *Nat. Commun.* **2021**, *12* (1), 3527.
(67) Jung, J.-H.; Kim, S. H.; Park, Y.; Lee, D.; Lee, J.-S. Metal-Halide Perovskite Design for Next-Generation Memories: First-Principles Screening and Experimental Verification. *Adv. Sci.* **2020**, *7* (16), 2001367.
(68) Meena, J. S.; Sze, S. M.; Chand, U.; Tseng, T.-Y. Overview of emerging nonvolatile memory technologies. *Nanoscale Res. Lett.* **2014**, *9* (1), 526.
(69) Gedda, M.; Yengel, E.; Faber, H.; Paulus, F.; Kreß, J. A.; Tang, M.-C.; Zhang, S.; Hacker, C. A.; Kumar, P.; Naphade, D. R.; Vaynzof, Y.; Volonakis, G.; Giustino, F.; Anthopoulos, T. D. Ruddlesden–Popper-Phase Hybrid Halide Perovskite/Small-Molecule Organic Blend Memory Transistors. *Adv. Mater.* **2021**, *33* (7), 2003137.

TOC

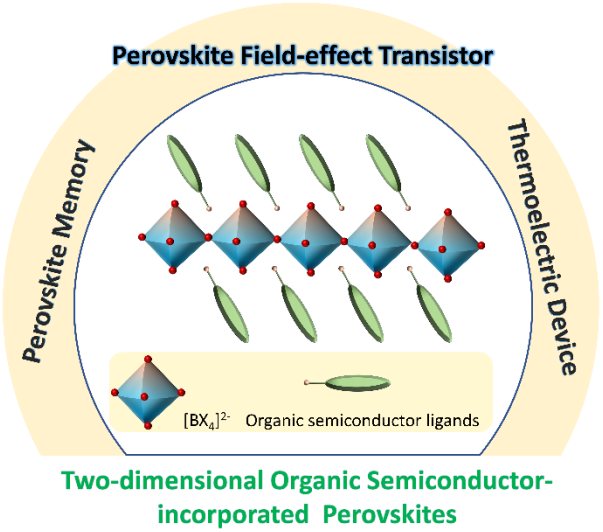
Perovskite Field-effect Transistor
Perovskite Memory
Thermoelectric Device
$[BX_4]^{2-}$ Organic semiconductor ligands
Two-dimensional Organic Semiconductor-incorporated Perovskites